NATO STANDARD

AEP-4367

THERMODYNAMIC INTERIOR BALLISTIC MODEL WITH GLOBAL PARAMETERS

Edition A Version 1

MAY 2015

NORTH ATLANTIC TREATY ORGANIZATION

ALLIED ENEGINEERING PUBLICATION

Published by the
NATO STANDARDIZATION OFFICE (NSO)

INTENTIONALLY BLANK

NORTH ATLANTIC TREATY ORGANIZATION (NATO)

NATO STANDARDIZATION OFFICE (NSO)

NATO LETTER OF PROMULGATION

17 May 2016

1. The enclosed Allied Engineering Publication AEP-4367, Edition A, Version 1, THERMODYNAMIC INTERIOR BALLISTIC MODEL WITH GLOBAL PARAMETERS, which has been approved by the nations in the NATO ARMY ARMAMENTS GROUP (NAAG), is promulgated herewith. The recommendation of nations to use this publication is recorded in STANREC 4367.

2. AEP-4367, Edition A, Version 1 is effective upon receipt.

3.

4. This publication shall be handled in accordance with C-M(2002)60.

Edvardas MAŽEIKIS
Major General, LTUAF
Director NATO Standardization Office

INTENTIONALLY BLANK

RESERVED FOR NATIONAL LETTER OF PROMULGATION

INTENTIONALLY BLANK

TABLE OF CONTENTS

CHAPTER 1 INTERIOR BALLISTIC GOVERNING EQUATIONS 1-1
CHAPTER 2 FORM FUNCTION EQUATIONS 2-1
ANNEX A LIST OF SYMBOLS A-1
ANNEX B BORE RESISTANCE DUE TO FRICTION AND ENGRAVING B-1
ANNEX C WEAPON RECOIL C-1
ANNEX D CLOSED VESSEL DATA REDUCTION D-1
ANNEX E DERIVATION OF THERMOCHEMICAL CONSTANTS E-1
ANNEX F INTERIOR BALLISTIC FITTING FACTORS F-1
ANNEX G GLOSSARY OF TERMS G-1
ANNEX H SELECTED BIBLIOGRAPHY H-1

INTENTIONALLY BLANK

CHAPTER 1 INTERIOR BALLISTIC GOVERNING EQUATIONS

1. The following equations constitute a mathematical model, a set of non-linear differential and algebraic equations, which simulate the one dimensional motion of a conventional, spin stabilized artillery projectile inside a gun tube. The physical mathematical modelling is accomplished mainly by:

a) including only the most essential forces,
b) approximating the burning of solid propellants, and
c) applying fitting factors to match the measured interior ballistic performance under standard and non-standard conditions.

AOP-51 is planned and will address how to implement the model and calibrate it against measured data. See Annex A for a list of symbols.

2. The equation of motion in the earth reference frame of the center of mass of the projectile is:

$$\dot{v}_p = \frac{\mathrm{d}v_p}{\mathrm{d}t} = \frac{A\left(P_b - f_R P_R\right)}{m_p}$$

where the area of the base of the projectile A including the appropriate portion of the rotating band is:

$$A = \frac{\pi}{4} D_b^2 \qquad \text{where:} \quad D_b^2 = \frac{GLR \cdot DG^2}{GLR+1} + \frac{DL^2}{GLR+1}$$

The pressure on the base of the projectile P_b including the approximate pressure gradient effect is:

$$P_b = \frac{\bar{P} + \dfrac{C_T f_R P_R}{3m_p}}{1 + \dfrac{C_T}{3m_p}}$$

and the bore resistance due to engraving and friction of the rotating band P_R is a function of the distance travelled with the resistance factor f_R being one during the engraving process ($x < x_{eng}$).

3. The velocity of the center of mass of the projectile is:

$$v_p = \int_0^t \dot{v}_p \mathrm{d}t$$

4. The breech pressure P_0 is:

$$P_0 = P_b + \frac{C_T}{2m_p}\left(P_b - f_R P_R\right)$$

5. The travel of the projectile is:

$$x = \int_0^t v_p \mathrm{d}t + \int_0^t v_{rp} \mathrm{d}t$$

and in the earth reference frame, the velocity of recoiling parts v_{rp} is always negative.

6. The mass fraction burning rate of the *i* th propellant is:

$$\frac{\mathrm{d}Z_i}{\mathrm{d}t} = \frac{S_i r_i}{V_{g_i}}$$

where the adjusted linear burning rate r_i is:

$$r_i = f_\beta f_{\beta T} \beta_i (\bar{P})^{\alpha_i} + k_v v_p$$

andV_{g_i} and S_i are computed using algebraic equations describing the geometry of the particular propellant grain(s) and k_v is the erosive burning coefficient and depends on the geometry of the grain. Typical values of k_v for single and seven perforation artillery propellants are 0.00002 and 0.00012 respectively.

7. The fraction of mass burned of the *i* th propellant is:

$$Z_i = \int_0^t \dot{Z}_i \mathrm{d}t$$

8. The adjusted force per unit mass of the *i* th propellant is:

$$F_i^{'} = f_{FT} F_i$$

9. The space-mean pressure $\bar{P}$ (Noble-Abel Law) is:

$$\bar{P} = \frac{T}{V_c}\left(\sum_{i=1}^{n}\frac{F_i' C_i Z_i}{T_{0_i}} + \frac{F_l C_l}{T_{0_l}}\right)$$

where the number of propellants is *n* and the volume available for gases is:

$$V_c = V_0 - \sum_{i=1}^{n} V_{p_i} + Ax - \sum_{i=0}^{n}\frac{C_i}{\rho_i}(1 - Z_i) - \sum_{i=0}^{n} C_i b_i Z_i - C_l b_l$$

and the temperature of the gases is given by:

$$T = \frac{\sum_{i=1}^{n}\frac{F_i' C_i Z_i}{\gamma_i - 1} + \frac{F_l C_l}{\gamma_l - 1} - E_{pt} - E_{pr} - E_p - E_{br} - E_r - E_h}{\sum_{i=1}^{n}\frac{F_i' C_i Z_i}{(\gamma_i - 1) T_{0_i}} + \frac{F_l C_l}{(\gamma_l - 1)\, T_{0_l}}}$$

where:

the energy loss due to the projectile translation E_{pt} is:

$$E_{pt} = \frac{m_p v_p^2}{2}$$

the energy loss due to projectile rotation E_{pr} is:

$$E_{pr} = \frac{\pi^2 m_p v_p^2}{4 T_w^2}$$

the energy loss due to propellant gas and unburned propellant motion E_p is:

$$E_p = \frac{C_T v_p^2}{6}$$

the energy loss for work against bore resistance due to engraving and friction of rotating band E_{br} is:

$$E_{br} = A\int_0^x f_R P_R \, \mathrm{d}x$$

where the resistance factor f_R is one during the engraving process ($x < x_{eng}$).

the energy loss due to recoil E_r is:

$$E_r = \frac{m_{rp} v_{rp}^2}{2}$$

the energy loss due to heat transfer to the chamber walls E_h is:

$$E_h = \int_0^t A_w h \left(T - T_c\right) \mathrm{d}t$$

where:

$$A_w = \frac{V_0}{A} \pi D_b + 2A + \pi D_b \, x$$

and

$$h = \lambda \bar{C}_p \bar{\rho} \bar{v} + h_0$$

where the Nordheim friction factor λ is:

$$\lambda = \left(13.2 + 4 \log \left(100 D_b\right)\right)^{-2}$$

$$\bar{v} = \frac{1}{2}\left(v_p + v_{rp}\right)$$

$$\bar{\rho} = \frac{\sum_{i=1}^{n} \int_0^t C_i \left(\frac{\mathrm{d}Z_i}{\mathrm{d}t}\right) \mathrm{d}t + C_l}{V_c}$$

Now $C_{pi} = \frac{F_i' \gamma_i}{\left(\gamma_i - 1\right) T_{0_i}}$, so that

$$\bar{C}_p = \frac{\sum_{i=1}^{n} \int_0^t \frac{F_i' \, \gamma_i C_i \left(\frac{\mathrm{d}Z_i}{\mathrm{d}t}\right)}{\left(\gamma_i - 1\right) T_{0_i}} \mathrm{d}t + \frac{F_l \, \gamma_l C_l}{\left(\gamma_l - 1\right) T_{0_i}}}{\sum_{i=1}^{n} \int_0^t C_i \left(\frac{\mathrm{d}Z_i}{\mathrm{d}t}\right) \mathrm{d}t + C_l}$$

Thus the temperature of the chamber wall T_c is:

$$T_c = \frac{E_h + f \, E_{br}}{C_{pw} \rho_w A_w D_w} + T_{0_w}$$

10. The equation of motion for the recoiling parts is:

$$\dot{v}_{rp} = -\frac{A_{br} P_0 - RR - A f_R P_R}{m_{rp}}$$

where:

$$\dot{v}_{rp} = 0 \text{ whenever } A_{br} P_0 < RR_0 + A f_R P_R$$

When:

$$A_{br}P_0 = RR_0 + A f_R P_R, \text{ then } t = t_{r_0}$$

11. The velocity of the recoiling parts v_{rp} in the earth reference frame is:

$$v_{rp} = \int_0^{t_r} \dot{v}_{rp} \mathrm{d}t_r \text{ , where } t_r = t - t_{r_0} .$$

INTENTIONALLY BLANK

CHAPTER 2 FORM FUNCTION EQUATIONS

1. The analysis for calculating burning rates from closed bomb firings and for calculating the change in mass versus time from burning rates in interior ballistic codes requires knowledge of the surface area and/or volume of a propellant grain as a function of depth burned. The assumption that the propellant burns normal (perpendicular) to all surfaces at the same rate, allows exact analytic equations to be derived for the complete surface area and volume as a function of the depth burned including the slivering phase if any occurs. These form functions should be used for both interior ballistic calculations as well as burning rate determination. All dimensions should be kept current during burning. See also Annex D.

2. The equations for the volume and surface area of a spherical grain type area:

$$V = \frac{1}{6}\pi D^3$$
$$S = \pi D^2$$

3. The equations for the volume and surface area of a Slab grain type are:

$$V = L \cdot WT \cdot WS$$
$$S = 2\left(L \cdot WS + L \cdot WT + WS \cdot WT\right)$$

4. The equations for the volume and surface area of a Single-perforation grain type are:

$$V = \frac{1}{4}\pi L\left(D^2 - P^2\right)$$
$$S = \pi\left(D \cdot L + P \cdot L + \frac{D^2}{2} - \frac{P^2}{2}\right)$$

5. The equations for the volume and surface area of a Seven-perforated grain type with equal webs and perforations where *x* is the distance burned are:

For: $x \le \frac{1}{2}w$

$$V = \frac{\pi}{4}(L - 2x)\left[(D - 2x)^2 - 7(P + 2x)^2\right]$$
$$S = \frac{2V}{(L - 2x)} + \pi(L - 2x)(D + 7P + 12x)$$

For: $x > \frac{1}{2}w$ (after slivering)

$$V = V_1 + V_2$$
$$S = S_1 + S_2$$

For: $\frac{1}{2}w < x < x_1$ (up to inner sliver burnout)

$$V_1 = \frac{3}{4}(L-2x)\left[2\sqrt{3}d^2 - \pi(P+2x)^2 + 24A_1\right]$$
$$S_1 = \frac{2V_1}{(L-2x)} + 3(L-2x)(\pi - 6\theta)(P+2x)$$

For: $x \geq x_1$

$$V_1 = S_1 = 0$$

For: $\frac{1}{2}w < x < x_2$ (also up to outer sliver burnout)

$$V_2 = \frac{1}{4}(L-2x)\left[\pi(D-2x)^2 - 6\sqrt{3}d^2 - 4\pi(P+2x)^2 + 24(A_1 + 2A_2)\right]$$
$$S_2 = \frac{2V_2}{(L-2x)} + (L-2x)\left[(\pi - 6\psi)(D-2x) + 2(2\pi - 3\varphi - 3\theta)(P+2x)\right]$$

For: $x \geq x_2$

$$V_2 = S_2 = 0$$

where:

$$\theta = \arccos\left(\frac{d}{P+2x}\right)$$

$$\psi = \arccos\left(\frac{5d - 2(P+2x)}{(D-2x)}\right)$$

$$\varphi = \arccos\left(\frac{3d - 2(P+2x)}{P+2x}\right)$$

$$A_1 = \frac{\theta}{4}(P+2x)^2 - \frac{d}{4}\sqrt{(P+2x)^2 - d^2}$$

$$A_2 = \frac{1}{8}\left[\varphi(P+2x)^2 - \psi(D-2x)^2 + 2\sqrt{3}d\sqrt{(3d-P-2x)(3d-D+2x)}\right]$$

6. The equations for the volume and surface area of a Slotted Stick Propellant grain type are:

$$V = 2L\left[(\pi-\theta)R^2 - (\pi-\alpha)r^2 - \left(\frac{1}{2}SW\cdot R\cos\theta - \frac{1}{2}SW\cdot r\cos\alpha\right)\right]$$

$$S = 2L\left[(\pi-\alpha)r + R\cos\theta - r\cos\alpha\right] \quad \text{(perforation)}$$

$$+2\left[(\pi-\theta)R^2 - (\pi-\alpha)r^2 - \left(\frac{1}{2}SW\cdot R\cos\theta - \frac{1}{2}SW\cdot r\cos\alpha\right)\right] \quad \text{(end)}$$

$$+2L(\pi-\theta)R \quad \text{(lateral)}$$

where:

$$\theta = \frac{\pi}{2} - \arccos\left(\frac{SW}{2R}\right),\ \alpha = \frac{\pi}{2} - \arccos\left(\frac{SW}{2r}\right),\ R = \frac{D}{2} \text{ and } r = \frac{P}{2}$$

and all dimensions are kept current during burning.

INTENTIONALLY BLANK

ANNEX A LIST OF SYMBOLS

A.1. LIST OF SYMBOLS FOR CHAPTER 1 ON INTERIOR BALLISTICS GOVERNING EQUATIONS

Symbol	Definition	Unit
A	Area of base of projectile including appropriate portion of rotating band	m^2
A_{br}	Area of breech face	m^2
A_w	Chamber wall area plus area of gun tube wall exposed to propellant gases	m^2
b_i	Covolume of *i* th propellant	m^3/kg
b_I	Covolume of igniter	m^3/kg
C_a	Speed of sound in air (340 m/s)	m/s
C_i	Initial mass of *i* th propellant	kg
C_I	Initial mass of igniter	kg
$\bar{C}_p$	Specific heat at constant pressure of propellant gas	J/(kg·K)
C_{pi}	Specific heat at constant pressure of *i* th propellant (over temperature range from T to T_0)	J/(kg·K)
C_{pw}	Heat capacity of steel of chamber wall	J/(kg·K)
C_T	Total mass of propellants and igniter	kg
d_i	Diameter of perforation in *i* th propellant grains	m
dt	Incremental time	s
dT	Incremental temperature	K
dx	Incremental distance travelled by projectile	m
D_b	Diameter of bore	m
D_i	Outside diameter of *i* th propellant grain	m
DG	Diameter of grooves	m
DL	Diameter of lands	m
D_W	Chamber wall thickness heated	m
E_{br}	Energy lost for work against bore resistance due to friction and engraving of rotating band	J
E_h	Energy lost due to heat transfer to the chamber and barrel walls	J
E_p	Energy lost due to propellant gas and unburned propellant motion	J
E_{pr}	Energy loss due to projectile rotation	J
E_{pt}	Energy loss due to projectile translation	J
E_r	Energy loss due to recoil	J
f	Fraction of work done against bore friction that preheats chamber	J
f_{FT}	Force temperature factor	1

Symbol	Definition	Unit
f_R	Down-tube resistance factor	1
f_β	Burning rate factor	1
$f_{\beta T}$	Burning rate temperature factor	1
F_a	Resultant axial force on projectile	N
F_f	Frictional force on projectile	N
F'_i	Adjusted force per unit mass of *i* th propellant	J/kg
F_i	Force per unit mass of *i* th propellant	J/kg
F_I	Force per unit mass of igniter propellant	J/kg
F_p	Propulsive force on base of projectile	N
g	acceleration due to gravity	m/sec^2
GLR	Groove-to-land width ratio	1
h	Heat transfer coefficient of Nordheim, Soodak, and Nordheim	W/(m^2·K)
h_0	Free convective heat transfer coefficient for air in gun tube	W/(m^2·K)
k_v	Erosive Burn Coefficient	1
L_i	Length of *i* th propellant grain	m
M	Mach number of the projectile with respect to the air (v_p /C_a)	1
m_p	Mass of projectile	kg
m_{rp}	Mass of recoiling parts	kg
n	Number of propellants	1
N_i	Number of perforations in *i* th propellant grain	1
$\bar{P}$	Space-mean pressure	Pa
P_a	Pressure in the ambient air (0.101 MPa)	Pa
P_b	Pressure on base of projectile	Pa
P_M	Maximum chamber pressure	Pa
P_0	Breech pressure	Pa
P_R	Resistive pressure of the bore due to friction and engraving	Pa
r_i	Linear burning rate of *i* th propellant	m/s
RR	Recoil resistance force	N
RR_0	Recoil resistance force at time $t = 0$	N
S_i	Surface area of partially burned *i* th propellant grain	m^2
S_{g_i}	Surface area of an unburned *i* th propellant grain	m^2
t	Time	s
t_r	Recoil time	s
t_{r_0}	Time of the beginning of recoil motion	s
T	Mean temperature of propellant gases	K
T_c	Temperature of chamber wall	K
T_{0_i}	Adiabatic flame temperature of *i* th propellant	K

Symbol	Definition	Unit
T_{0_i}	Adiabatic flame temperature of igniter propellant	K
T_{0_w}	Initial temperature of chamber wall	K
T_S	Temperature of unburned solid propellant	K
T_W	Twist of rifling	calibers/turn
$\bar{v}$	Mean gas velocity	m/s
v_m	Velocity of projectile at muzzle of barrel	m/s
v_p	Velocity of projectile	m/s
$\dot{v}_p$	Acceleration of projectile	m/s^2
v_{rp}	Velocity of recoiling parts	m/s
V_c	Volume behind projectile available for propellant gas	m^3
V_{g_i}	Volume of an unburned *i* th propellant grain	m^3
V_0	Volume of empty cannon chamber	m^3
V_{p_i}	Volume of parasitics associated with *i* th propellant	m^3
W	External work done on projectile	J
x	Travel of projectile	m
x_{eng}	Travel of projectile at completion of rotating band engraving	m
x_m	Travel of projectile when base reaches muzzle	m
x_{rp}	Travel of recoiling parts	m
Z_i	Fraction of mass burned of the *i* th propellant	1
$\dot{Z}_i$	Mass fraction burning rate for *i* th propellant	1/s
α_a	Ratio of specific heats for air (1.4)	1
α_i	Burning rate exponent for *i* th propellant	1
β_i	Burning rate coefficient for *i* th propellant	$m/(s \cdot Pa^{\alpha})$
γ_i	Ratio of specific heats for *i* th propellant	1
γ_I	Ratio of specific heats for igniter	1
λ	Nordheim friction factor	1
$\bar{\rho}$	Mean gas density	kg/m^3
ρ_i	Density of *i* th propellant	kg/m^3
ρ_w	Density of chamber wall steel	kg/m^3

A.2. LIST OF SYMBOLS FOR CHAPTER 2 ON FORM FUNCTION EQUATIONS

Symbol	Definition	Unit
d	Distance between perforation centers	m
D	Grain diameter	m
L	Grain length	m
P	Perforation diameter	m

Symbol	Definition	Unit
R	Grain radius	m
r	Perforation radius	m
S	Surface of grain	m^2
SW_i	Slot width	m
S_1	Surface of inner sliver	m^2
S_2	Surface of outer sliver	m^2
V	Volume of grain	m^3
V_1	Volume of inner sliver	m^3
V_2	Volume of outer sliver	m^3
WL_i	Slab length	m
WT_i	Slab thickness	m
WS_i	Grain width	m
w	Web	m
x	Distance burned	m
x_1	Distance burned when inner sliver burns out	m
x_2	Distance burned when outer sliver burns out	m

ANNEX B BORE RESISTANCE DUE TO FRICTION AND ENGRAVING

B.1. INTRODUCTION

1. The group of differential equations that governs the internal ballistic cycle consists of the energy equation, the impulse equation, the equation of motion and the burning law. The form function is included in the burning law. The equation of energy conservation is considered to be the main equation of an interior ballistic problem. It gives the rules for how energy is liberated by a propelling charge, and ways in which this energy is absorbed and changed.

2. One of the energy losses treated in the interior ballistic trajectory model is due to the work required to engrave the rotating band and overcome friction between the band and gun tube. The physics of the process and magnitudes of the forces involved are not well defined and the following discussion outlines the assumptions contained in the present trajectory model.

3. The projectile is restrained from moving until a pre-defined shot-start pressure is achieved. A nominal value of 15 to 20 MPa for rifled barrels is generally used based on limited testing and theoretical considerations. The inclusion of resistance pressure in the pressure gradient term helps ease the transition from shot-start to normal projectile motion. A linear increase in engraving resistance versus distance travelled is then assumed until the point of maximum compression. The distance to maximum engraving pressure is calculated using rotating band/forcing cone interference geometry and compensates for the presence of cannelures and obturating bands. The resistance then decreases rapidly with travel until band is fully engraved. Good correspondence to the reference data from test firings has been achieved using a smoothly constructed profile of the resistance pressure so that after engraving the profile decreases as relation to 1/x. The maximum engraving pressure can be estimated by using Gabot's approximation [1] and empirical evidence or by analyzing from pressure-time curve $p(t)$.

B.2. LOADS APPEARING IN INTERIOR BALLISTIC CYCLE

B.2.1. Resistive forces

1. The resistive force $F_R = A\, f_R P_R$ is integrated into the interior ballistic model through the equation of motion whose general form is as follows:

(B.1.)
$$\dot{v}_p = \frac{\mathrm{d}v_p}{\mathrm{d}t} = \frac{A(P_b - f_R P_R)}{m_p}$$

2. The solution of the interior ballistic equation group at each step requires that the resistive forces can be defined (predicted) at each step as the projectile advances down the tube. In a firing sequence, the projectile motion proceeds under the influence of propulsive and resistive forces. The projectile is forced forward, with obturation provided by a rotating band which is engraved by the rifling as the projectile moves into the barrel. The resistive forces can be divided as follows:

a) the force required for the engraving of the rotating band,
b) the resistance from the projectile motion through the barrel where a metal-metal press fit situation exists,
c) propulsive forces used for angular acceleration,
d) the frictional sliding resistance from the resolved force normal to the edge of the land.

3. In designing the rotating bands and grooves, care must be taken that the different stresses can be supported. The following definition is also used when evaluating the loads for the FEM (Finite Element Method) analysis of the projectile during the interior ballistic phase.

4. The pressures between the rotating band and barrel should be treated as if they were uniform and axial-symmetric. In actuality, rifling may create a non-uniform stress distribution in both barrel and rotating band at their interface but modeling of these is above the level of this text.

5. The treatment here is based on [2], which is a further development of the modeling of the works of [3], [4], and [5].

6. The problem is to develop a method to calculate the resistive force as projectiles advance down the gun tube. The forces in rifled guns can be derived by examining the force components that affect the rotating band
a) in engraving phase and
b) after engraving.

B.2.2. Wear process of the rotating band

1. Rotating bands are manufactured from copper, copper alloys, soft iron or plastic and are usually pressed into a corresponding groove in the projectile body and finally machined down to their finished size. The outside diameter of the band is somewhat greater than the so called big caliber of the bore, and in this way it is assured that after engraving into the grooves, the profile of the grooves is completely filled and the rotating bands provide a good seal for the propellant gases.

2. Within a few centimeters from the origin of the rifling, a thin lubrication film of molten metal is produced on the surface of the band. The entire travel of the projectile down the bore is lubricated sliding and, the band is wearing by melting on the surfaces

where a metal-metal press fit situation exists [6]. The thickness of the liquid copper film, supported on the sliding surface is very small and the greater part of the melted copper alloy is squeezed out. This results in better heat transfer through the liquid film because of its reduced thickness and further melting of the rotating bands and consequently faster rotating band wear. By choosing the materials with respect to their sliding characteristics and heat resistance the frictional work can be kept as low as possible for high ballistic ratings and a high rate of fire, so that the conditions that preserve the tube can be achieved.

3. During the engraving process through the forcing cone the rotating band must be swaged to the bore diameter and engraved by the rifling, Fig. B. 1. The result of the initial process is required to enable the gun system to build up a relatively large starting pressure. It should be noted that the magnitude of the resistance forces during the engraving process will depend on the ramming technique and the wear state of the cannon in the forcing cone region. The ignition system of the propelling charge consists of fast burning propellants. Proper ignition requires that the engraving process delays the projectile travel until the burning rate and gas pressure have reached the optimum values. During sliding through the tube the lands deform further and because of the friction the lands wear on outer edges. The final shape of the rotating band at exit from the tube depends on the rifling type (Fig. B. 2.).

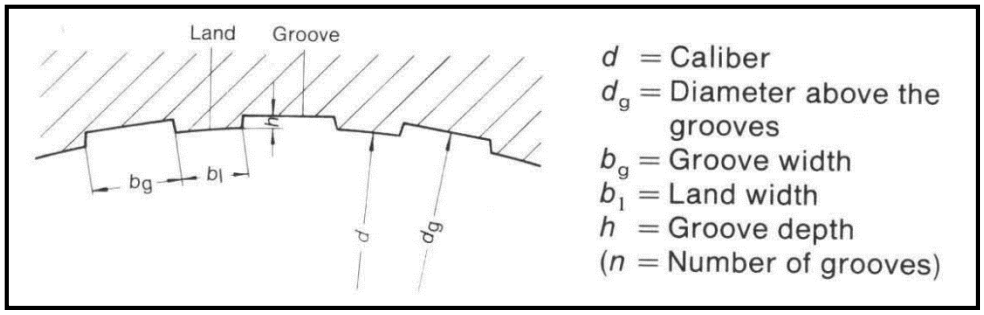

Fig. B. 1. Cross section through a rifled bore [7].

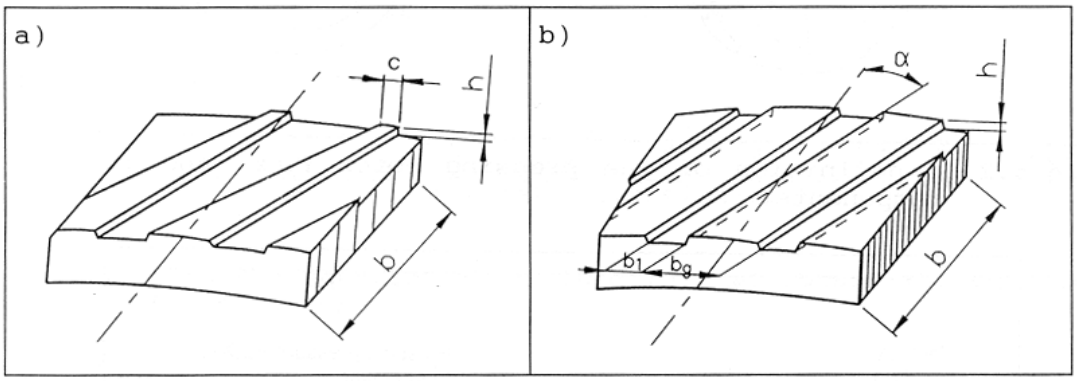

Fig. B. 2. Details of rotating band, after engraving through a) parabolic and b) constant rifling [2].

4. Deformation of the rotation band during engraving is a fast process. The initial sliding is a dry sliding and generally wear problems can be traced to this very short period of dry sliding. Typical numerical values for the friction coefficient $\mu(x)$ in lubricated phase lie between 0.1 - 0.4 depending on the hydrodynamic properties of the melted layer. The value is highest at the beginning and decreases towards the end of the tube. For example, the values of $\mu(x)$ for projectiles of the 155 mm M185 howitzer, based on laboratory testing, have been about 0.15 after the travel of 150 mm from the origin of the rifling [5].

B.2.3. Equilibrium equations

B.2.3.1. Engraving process

1. The stress fields present during the engraving process are complex and probably cannot be adequately described analytically, particularly with regard to the state of stress experienced by the rotating band while undergoing its gross plastic deformation. The problem becomes more tenable by the use of a combined analytical-experimental description of the process.

2. We consider a rather idealized description of the physical situation which exists at the beginning of the engraving process as depicted in Fig. B. 3. The engraving force F_R behind the projectile base is the product of engraving pressure and the cross-sectional area of the tube $P_R A$. The radial compression force F_P acting on the rotating band is normal to the surface of forcing cone. The frictional force is defined as the normal force multiplied by the friction coefficient $\mu(x)$. The engraving length x_{eng} is the travel distance of the projectile from the origin to the point of full height of rifling. (Fig. B. 3.).

3. As the projectile advances in the forcing cone engraving more of the rotating band the pressure of propellant gases behind the projectile increases. The forces retarding this advance are lateral components of F_P and the frictional force μF_P. Therefore the resistive force:

(B.2.) $$F_R = A f_R P_R = F_P (\sin\beta + \mu\cos\beta)$$

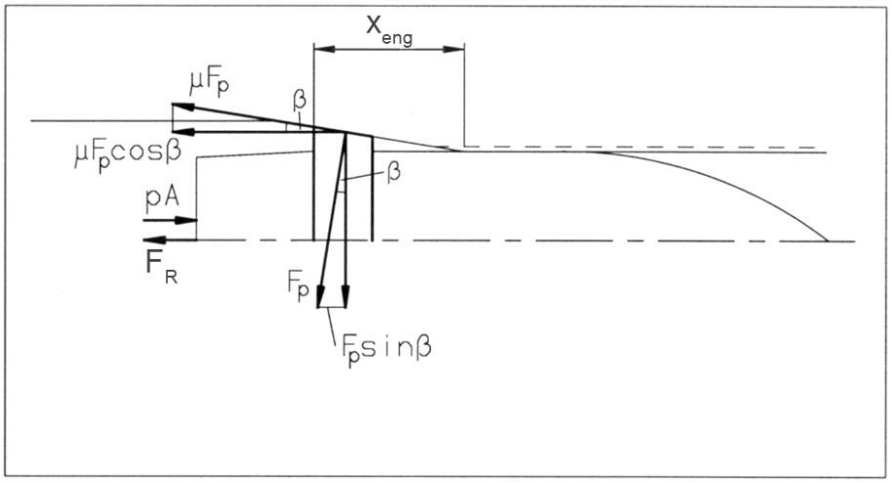

Fig. B. 3. Initial Engraving Geometry (β = half angle of the forcing cone, x_{eng} = engraving length).

2.3.2. After engraving process

1. After the rotating band is deformed, the forces acting on the projectile are:
   - rifling force $R(x)$ (Fig. B. 4.) and
   - radial pressing force $F_P(x)$ (Fig. B. 5.).

2. The direction of the rifling force $R(x)$ is normal to the edge of the land. The forces $R(x)$ and $F_P(x)$ are understood to be the totals of all tangential guide and radial pressing forces transmitted between the lands of the bore surface and the rotating band. The rifling force $R(x)$ causes the projectile to rotate, and along the tube axis it is dependent on the type of the rifling curve of the gun.

3. The frictional force is defined as the normal force multiplied by the friction coefficient $\mu(x)$. By summation of the x-components of the rifling force $R(x)$ and the pressing force $F_P(x)$ the equation of translation motion becomes

(B.3.) $$m_p \frac{\mathrm{d}v}{\mathrm{d}t} = P_b A - R(x)\left(\sin\alpha(x) + \mu\cos\alpha(x)\right) - \mu F_P \cos\alpha(x)$$

By solving for A $f_R P_r$ in eq. B. 1, it is obtain for the resistive force

(B.4.) $$F_R = A f_R P_R = R(x)\left(\sin\alpha(x) + \mu\cos\alpha(x)\right) - \mu F_P \cos\alpha(x)$$

The rifling force $R(x)$ can be solved from the equation of rotational motion. The equilibrium of moments about x-axis yields

(B.5.) $$I_x \frac{\mathrm{d}\omega}{\mathrm{d}t} = R(x)\left(\cos\alpha(x) - \mu(x)\sin\alpha(x)\right)\frac{d}{2} - \mu(x) F_P(x) \sin\alpha(x) \frac{d}{2}$$

The angular velocity and angular acceleration are defined as:

(B.6.) $$\omega = \frac{2}{d} v \frac{\mathrm{d}y}{\mathrm{d}x}$$

(B.7.) $$\frac{\mathrm{d}\omega}{\mathrm{d}t} = \frac{2}{d}\frac{\mathrm{d}v}{\mathrm{d}t}\frac{\mathrm{d}y}{\mathrm{d}x} + \frac{2}{d}v^2\frac{\mathrm{d}^2y}{\mathrm{d}x^2}$$

By inserting into B. 5, it is obtain

(B.8.) $$R(x) = \frac{I_x\left(\frac{2}{d}\right)^2\left(\frac{\mathrm{d}v}{\mathrm{d}t}\frac{\mathrm{d}y}{\mathrm{d}x} + v^2\frac{\mathrm{d}^2y}{\mathrm{d}x^2}\right) + \mu(x)F_P(x)\sin\alpha(x)}{\cos\alpha(x) - \mu(x)\sin\alpha(x)}$$

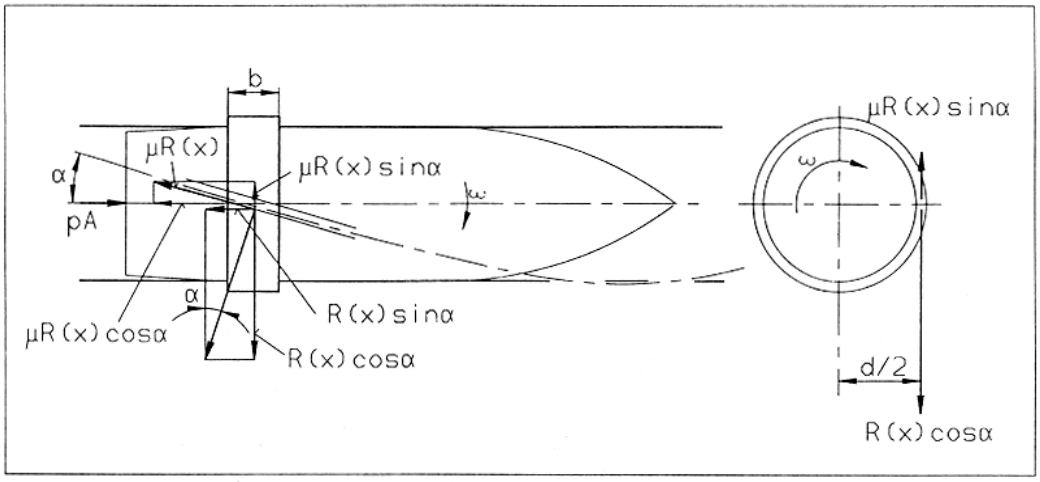

Fig. B. 4. Definition of the rifling force *R(x)* and its components [2].

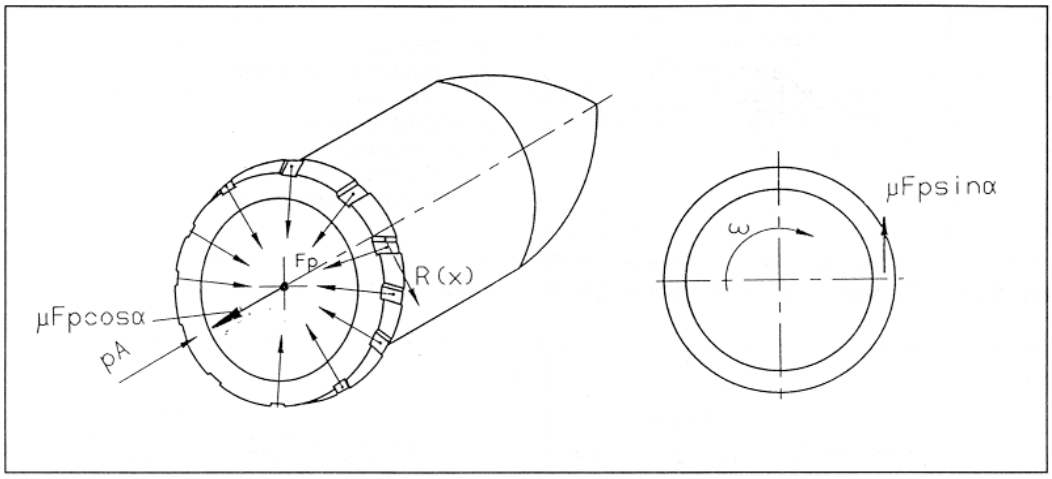

Fig. B. 5. Definition of the pressing force $F_P(x)$ and its components [2].

4. The pressing force $F_P(x)$ is the product of compressing pressure $P_P(x)$ and surface area of rotating band being compressed defined as:

(B.9.) $$F_P(x) = P_P(x)\frac{N\, b_l\, b}{\cos\alpha}$$

where b_l and b are defined in Figs. B. 1. and B. 2.

5. Approximation of the pressing pressure P_P versus projectile travel x is based on construction as depicted in Fig. B. 3. From the origin to approximately the maximum value $P_{P\,max}$ the dependence is assumed to be linear (Fig. B. 6.). After engraving, the pressing pressure $P_P(x)$ decreases gradually towards the end of the tube. The top of the curve may be approximated by a smooth curve when implementing the pressing pressure $P_P(x)$ in a simulation. By inserting the definition of pressing pressure $P_P(x)$ (Fig. B. 6.) in the equations of $R(x)$ and $A\, f_R\, P_R(x)$ in the equation of motion it is obtained the equation for the friction force as a function of projectile travel x, as depicted in Fig. B. 7. It should be noted that Figs. B. 6. and B. 7. do not reflect the shot start pressures.

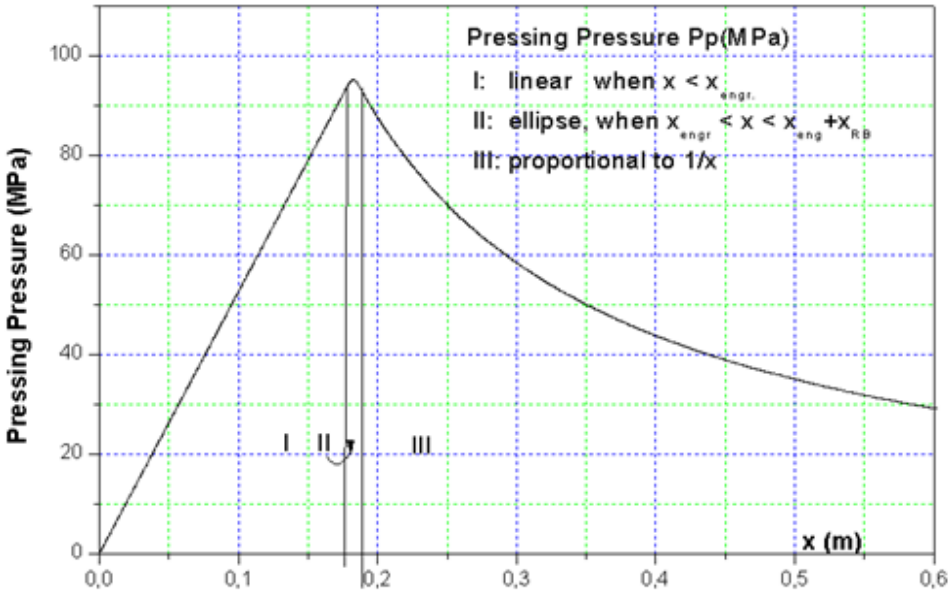

Fig. B. 6. Approximation of the pressing pressure $P_P(x)$.

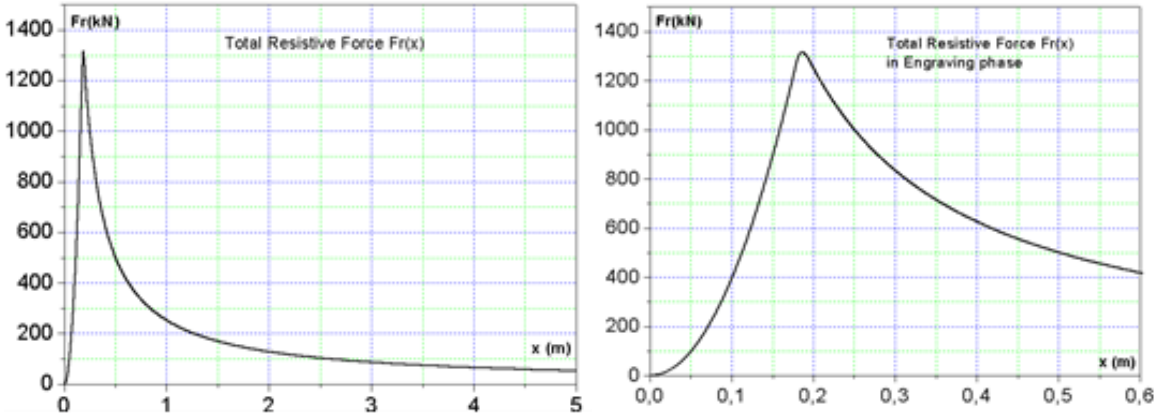

a) b)

Fig. B. 7. The result lateral resistive force a) as function of travel length and b) at beginning of tube.

2.3.3. Numerical approximation of $P_{P\,max}$

1. Numerical approximation for the maximum pressing pressure $P_{P\,max}$ and furthermore for the pressing force $F_P(x)$ can be approximated using equation for maximum value as below:

(B.10.) $$P_{P\,max} = Y\frac{\tilde{A}}{A}\left(\sin(\beta)+\mu\cos(\beta)\right)\cos(\alpha)$$

where strain of rotating band for determination of Y is defined as

(B.11.) $\text{Strain} = \left(d_{b(0)} - d_l\right) / \left(d_{b(0)} - d_{b(s)}\right)$

and $\tilde{A}$ is defined as

$$\tilde{A} = N\, b_l\, b$$

2. Typical values for Y are 200-350 MPa. The material data for different rotating band materials is tabulated in [8].

B.3. LIST OF SYMBOLS

Symbol	Definition	Unit
A	Area of base of projectile including appropriate portion of rotating band	m^2
$\tilde{A}$	Area of lands	m^2
b	Band width	m
b_l	Land width	m
$d_{b(0)}$	Outside diameter of band	m
$d_{b(s)}$	Band seat diameter	m
d_g	Diameter above the grooves	m
d_l	Diameter between lands	m
f_R	Down-tube resistance factor	1
F_P	Radial compressive force	N
F_R	Resistive force of the bore due to friction and engraving	N
h	Groove depth	m
I_x	Moment of inertia about the longitudinal axis	$kg \cdot m^2$
m_p	Mass of projectile	kg
n	Number of grooves	1
N	Number of lands	1
P_b	Pressure on base of projectile	Pa
P_P	Pressing pressure	Pa
P_R	Resistive pressure of the bore due to friction and engraving	Pa
$R(x)$	Rifling force	N
r_p	Radius of projectile	m
x	Displacement in x direction	m
x_{eng}	Engraving length	m
Y	Yield stress	Pa
y	Displacement in y direction	m
α	Angle of rifling	rad
β	Half angle of forcing cone	rad
$\mu(x)$	Friction coefficient	1
ω	Angular velocity	rad/s

4. REFERENCES

1. Serebryakov, M. E. Internal Ballistics, Translated by V. A. Nekrassoff, Washington, D.C.: Catholic University of America, 1950, p. 601.

2. Tuomainen, A. The Thermodynamic Model of Interior Ballistics, Academic Dissertation, Applied Physics Series No. 205 Acta Polytechnica Scandinavica, University of Helsinki, Department of Physics, 1996.

3. Witt, W. and Melchior, E. Thermodynamic Model of Interior Ballistics (Part I). *Wehrtechnik*, 6, 1974, p. 222-225.

4. Witt, W. and Melchior, E. Thermodynamic Model of Interior Ballistics (Part II). *Wehrtechnik*, 8, 1974, p. 288-292.

5. Montgomery, R. S. Projectile lubrication by melting rotating bands, Technical Report, Benet Weapons Laboratory, April, 1976, p. 21.

6. Montgomery, R. S. Wear of projectile rotating bands, Technical Report, Benet Weapons Laboratory, March 1985, p. 28.

7. Handbook on Weaponry, Düsseldorf: Rheinmetall, 1982, p. 752.

8. AMCP 706-247, Engineering Design Handbook, Ammunition and Explosives Series, Section 4, Design for Projection, Washington, D.C.: Headquarters, U.S. Army Materiel Command, July 1964.

5. ADDITIONAL BIBLIOGRAPHY

9. Germershausen, R., Witt, W. and Melchior, E. Wehrtechnik, 7, 1971, p. 281-288.

10. Mader, C. L., Numerical Modeling of Detonations, Berkeley: University of California Press, June 1979, p. 485.

11. Melchior, E. and Witt, W. Some theoretical considerations on Improving the Internal Ballistic Performance of Guns. *Propellants and explosives*, 1, 1976, p. 114-119.

12. Montgomery, R. S. Surface Melting of Rotating Bands, Technical Report, Benet Weapons Laboratory, November, 1975.

13. Montgomery, R. S. Muzzle wear of cannon, Technical Report, Benet Weapons Laboratory, February, 1975.

ANNEX C WEAPON RECOIL

1. The basis function of the recoil mechanism is to permit the gun barrel to move in the direction opposite that of the projectile, while permitting the gun mount or tank or other carrier to remain in position, and limit the distance of the recoil of the gun barrel.

2. A recoil mechanism is preloaded using springs and/or oil pressure. Once the rearward force on the gun barrel exceeds the preload force, the gun barrel begins to move backwards. The time of beginning of the recoil motion is called t_{r_0}. The force exerted by the recoil mechanism increases approximately linearly until well after the time at which the projectile exits the gun. The time of projectile exit is t_{r_0} plus the "rise time" of the recoil mechanism.

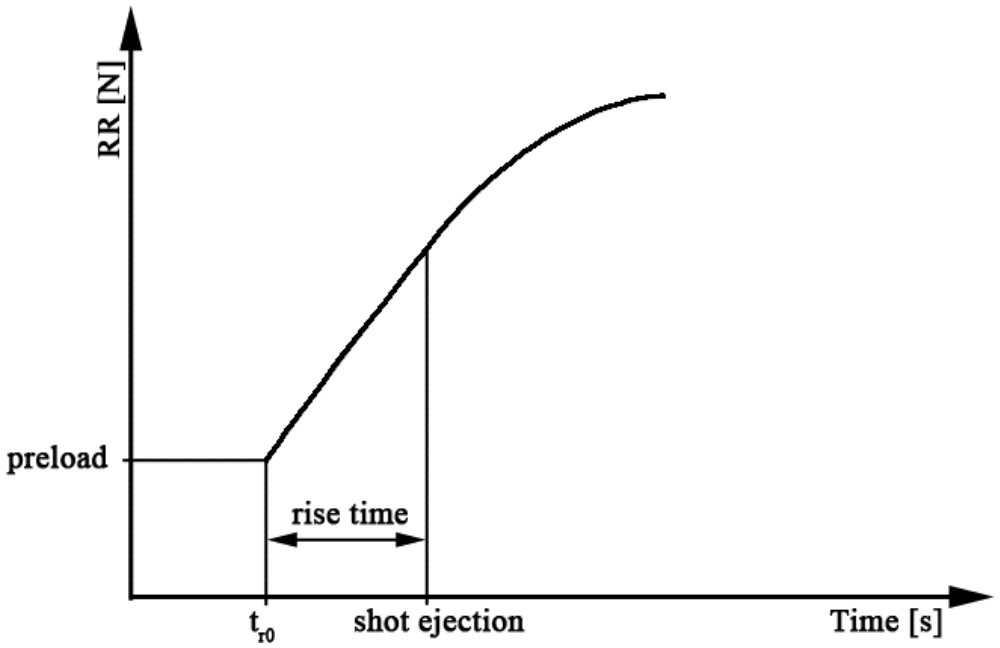

Figure C. 1. Weapon recoil resistance force *RR* vs. time *t*.

INTENTIONALLY BLANK

ANNEX D CLOSED VESSEL DATA REDUCTION

1. The propellant burning-rate coefficient and exponent required in the mass fraction burning in the rate-equation may be obtained by burning a small quantity of propellant in a closed vessel and recording the pressure versus time trace. The following articles:

- "The Closed Bomb Technique for Burning Rate Measurement at High Pressure" by Juhasz, A. A. and Price, C. F. found in the Experimental Diagnostics in Combustion of Solids, Vol. 63 of AIAA Progress in Astronautics and Aeronautics,
- "Gun Propellants" by L. Stiefel found in Interior Ballistics of Guns, Vol. 66 of AIAA Progress in Astronautics and Aeronautics,

provide good descriptions of the general approach. STANAG 4115 Definition and determination of ballistic properties of gun propellants describes the current standard NATO procedure for conduction closed-vessel testing.

2. Data reduction is accomplished through an inverse solution of the mass fraction burning rate, fraction mass burned and space-mean pressure equations. The "best-fit" burning rate coefficient and exponent are derived by fitting the computed pressure versus time to the actual pressure versus time as noted in Annex C of the STANAG 4115. As noted in "The closed bomb technique for burning rate measurement at high pressure" by Juhazs, A. A. and Price, C. F. the portion of the curve between 20 % and 80 % of maximum pressure is used in this procedure. Other adjustments required include accounting for heat loss to the closed vessel and the energy contribution of the igniter.

INTENTIONALLY BLANK

ANNEX E DERIVATION OF THERMOCHEMICAL CONSTANTS

1. The thermochemical constant required, for any propellant are force constant, the caloric value, the covolume, the ratio of specific heats and the adiabatic flame temperature. The first three constants are defined either experimentally or theoretically, the last two can only be determined theoretically. Assuming the Noble-Abel equations of state, by firing a series of charges of different masses in closed vessels, recording the maximum pressures, plotting and fitting a straight line to those points, the force and covolume can be determined. The gradient of the line gives the force factor and intercept of the line with y-axis give the covolume.

2. The theoretical method is via thermochemical equilibrium computer programs. The input required for these consists of the chemical composition of each constituents of the propellant, the heat formation of the propellant and elemental formula of each constituent of the propellant. The methods of calculating the constants are described in the STANAG 4400 Derivation of thermochemical values for interior ballistic calculation. STANAG 4400 standardizes the methods of calculating the constant by Hirschfelder-Sherman, Corner BLAKE and BAGHEERA. At high pressures above about 400 – 500 MPa, it is preferable to use the Amagat approximation as in the French code BAGHEERA.

INTENTIONALLY BLANK

ANNEX F INTERIOR BALLISTIC FITTING FACTORS

1. The four fitting factors f_β, f_R, $f_{\beta T}$ and f_{FT} are included in the Thermodynamic Interior Ballistic Model with Global Parameters. They may be used to cause the muzzle velocities and peak pressures predicted by the model to match observed muzzle velocities and peak pressures as projectile weight and propellant ambient temperature are varied. The first pair of factors: f_β and f_R, are used to match the observed peak pressure and muzzle velocity when firings are done at ambient temperature (294 K). Then the second pair of factors: $f_{\beta T}$ and f_{FT} is used to match the observed peak pressures and muzzle velocities as firings are performed at different propellant ambient temperatures. This process is illustrated in the following table:

Fitting to	Fitting Data as a Function of	
	Propelling Charge	Propellant Temperature
Maximum Chamber Pressure	Burning Rate Factor: f_β	Burning Rate Temperature Factor: $f_{\beta T}$
Muzzle Velocity	Down-tube Resistance Factor: f_R	Force Temperature Factor: f_{FT}

2. It is understood the use of a factor f_β to modify the value of the propellant burn rate coefficient does not imply that the measured coefficient is necessarily inaccurate, just that peak pressure is a strong function of burn rate coefficient, so that f_β is a powerful tool for matching peak pressures. Similarly f_R as it addresses down-tube resistance. Aids matching muzzle velocity. But utilizing resistance variations does not imply that the resistances have not been measured accurately. The same apply in temperature factors also.

INTENTIONALLY BLANK

ANNEX G GLOSSARY OF TERMS

1. Reference frame and Axis

Interior ballistic trajectories are treated as one-dimensional motion of the projectile along the axis defining the center of the gun's bore, and that axis is assumed to be horizontal. The origin of projectile motion is taken to be at origin of rifling.

2. Ignition of Propellant

The combustible material used to ignite the propelling charge is assumed to be fully burnt at the start of the simulations; the resulting chamber pressure is also assumed to be sufficient to support burning of the charge.

3. Burning Rate of Propellant

For a given propellant combustion at a given initial temperature, the rate of burning will be primarily a function of the pressure under which the reactions proceeds. Other factors such as the motion of the propellant grains relative to the gases and erosive burning constant k_v, etc., can also influence the burning rate. The burning rate coefficient β and index α used to relate burning rate to pressure are shown in Chapter 1, paragraph 6 of this AEP.

4. Force of Propellant

The force of the propellant is proportional to the energy released by a unit mass of propellant at a specific temperature. The force can be determined experimentally using closed chamber tests or estimated from thermochemical data when available.

5. Bore Resistance

The combined resistance due to engraving the rotating band and the friction between the moving projectile and the gun tube is called bore resistance. This resistance is a function of the displacement of the projectile with the maximum resistance occurring at the point of full engraving followed by a rapid decline to a steady-state value representing the friction between the rotating band and the gun tube.

6. Pressure Gradient

A difference in pressure exists between the breech face and projectile base which must be taken into account in the equations of motion. The expression chosen to represent the difference between the space-mean pressure and the pressure on the base of the projectile is a variant of the Lagrange-Piobert form and includes the resistance pressure in order to facilitate the transition from the shot start.

7. Fitting

To compensate for the approximations in the Thermodynamic Interior Ballistic Model with Global Parameters, fitting factors may be applied in order to create correspondence between the computed and the observed values of maximum chamber pressure and muzzle velocity. It is acknowledged that these fitting factors encompass corrections due to uncertainties in

a) the reduction of closed vessel data,
b) thermochemistry,
c) tube resistance, etc.

ANNEX H SELECTED BIBLIOGRAPHY

Title	Topic
Serebryakov, M. E. Internal Ballistics, Translated by V. A. Nekrassoff, Washington, D.C.: Catholic University of America, 1950, p. 601	Basic interior ballistic text
Hunt, F. R. W. Internal Ballistics, New York: Philosophical Library, 1951, p. 311	Basic interior ballistic studies
The Simulation of Interior Ballistic Performance of Guns by Digital Computer Program. Paul G. Baer and Jerome M. Frankle, Dec 1962, BRL Report No. 1183	Definition and derivation of original model
Engineering Design Handbook, AMCP 706-150, Washington, D.C.: HQ USAMC, Feb 1965	US Army interior ballistic design guide
Determination of Muzzle Velocity Charges Due to Nonstandard Propellant Temperature Using an Interior Ballistic Computer Simulation, James F. O'Bryon, Sep 1972, BRL Memorandum Report No. 2225	First generation propellant temperature model.
Development of a Dynamic Bore-Friction Model for Guns and Mortars and Its Conceptual Application to Early-Round And Gun Erosion Inaccuracies, J. Stals Material Research Laboratory Report No. 573, Maribirmong, Victoria, Australia, Oct 1974	On the calculation of profiles of resistance versus travel in guns
Measurement of Interior Ballistic Performance Using FM/FM Radio Telemetry Techniques, J. W. Evans, BRL Technical Report, BRL-TR-2699, December 1985	Description of measurements of profiles of resistance versus travel in guns
IBHVG2 - A User's Guide. Ronald D. Anderson and Kurt D. Fickie. BRL Technical Report BRL-TR-2829, July 1987.	User's Guide for IBHVG2 Interior Ballistics Code
Thermal Effects of Propellant Gases in Erosion Vents and in Guns, Nordheim, L. W., Soodak, H. and Nordheim, G. National Defence Research Report Number A-262 (OSRD no. 3447) Division 1, March 1944, p. 218	Source for the relevant empirical formula
Development of General Form - Functions For Multiperforated Cylindrical Propellant Grains, Lynn, F. R., USA ARDC Memorandum Report ARBRL-MR-03014, April 1980, AD A086104	How to construct equations for multiperforated cylindrical propellant grains.

AEP-4367 (A)(1)